AIAA 81-4152

Wind-Tunnel Measurements of Sabot-Discard Aerodynamics

Edward M. Schmidt*
U.S. Army Ballistic Research Laboratory, Aberdeen Proving Ground, Md.

The paper addresses the flowfield around a fin-stabilized, hypervelocity projectile during the sabot-discard process. The mutual interference of the flows around the flight body and three sabot components is examined through wind-tunnel tests conducted at a freestream Mach number of 4.5. Since it was not practical to attempt the actuation of all three sabot components, the flowfield was simulated by using splitter plates to develop reflection surfaces along planes of symmetry. The data show the effects of multiple shock interactions, shock/boundary-layer interactions, and the variation in aerodynamic loadings as the sabot discard proceeds.

Introduction

A SABOT (Fig. 1) is required to launch the current family of antiarmor, kinetic energy projectiles. Within the bore, the sabot provides gas sealing, structural support, and reduced sectional density. However, once free of the gun tube, the sabot must be discarded in order to permit unconstrained, low-drag flight to the target. Typically, the sabot is divided into three or more components along axial planes. These components separate from the projectile under the action of elastic, inertial (gyroscopic), and aerodynamic loads. During this separation, both mechanical and gasdynamic perturbations may result in alteration of the projectile trajectory.

It has been demonstrated[1-3] that aerodynamic interference can be a significant source of launch disturbance. The perturbation is strengthened by geometric asymmetry in the discard pattern and by extended periods of flight of the sabot segments in close proximity to the projectile. The details of this hypervelocity, three-dimensional interference flowfield are not well understood.

The present paper describes the results of an experimental progam to investigate the aerodynamics of sabot discard. A wind-tunnel model was fabricated to a representative sabot/projectile design. Tests were conducted at the NASA Langley Unitary Plan Facility to measure pressure distributions on both the projectile and sabot. Based on the wind-tunnel data, design modifications are suggested to improve discard.

Model Design and Test Procedure

Since it was not practical to attempt a test program incorporating multiply actuated sabot components, a system was required to simulate the flowfield about the configuration of interest but using only one driven sabot segment. Splitter plates were selected as a feasible means of generating reflecting planes of symmetry. Splitter plates have been used to test the dynamics of half-bodies[4] and to examine the flowfield about and mutual interference between two bodies.[5] The resulting data were shown to agree well with full-body results. In the present tests, the splitter plate technique is applied to simulate a trilaterally symmetric flow.

The configuration selected for testing is a three-segment sabot (Fig. 2). The 120 deg included-angle sabot component is positioned along the plane of symmetry of the splitter plates and projectile centerbody. The splitter plates act as reflecting surfaces along planes of symmetry in the trilaterally symmetric flowfield. In order to use this technique, only discard from smooth-bore guns can be considered since any precessional, rolling, or yawing motion would destroy the symmetry of the flow along 120 deg planes. As a means of checking the accuracy of this simulation, a three-sabot configuration (Fig. 3) was also fabricated.

The projectile was a stainless-steel cone cylinder having a diameter of 50.8 mm, a length-to-diameter ratio of 10.5, and a 30 deg total included-angle conical nose. Fifty static pressure orifices were positioned on the surface between the 120 deg planes of symmetry. With the exception of four orifices distributed about the conical forebody, no taps were located outside of these meridians. The splitter plates were fabricated from 6.35 mm thick stainless-steel plates having dimensions of 0.41×0.44 m. The leading edges of the splitter plates were chamfered at a 15 deg angle. No pressure taps

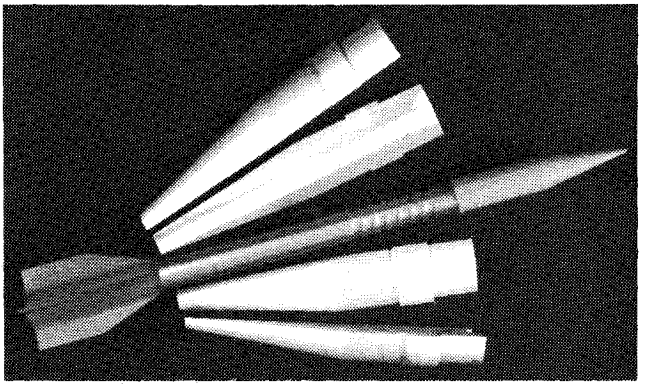

Fig. 1 Typical projectile and (four) sabot components.

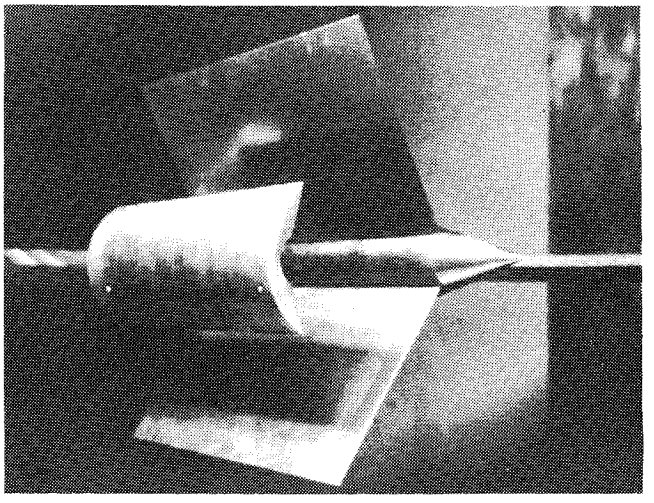

Fig. 2 Sabot and projectile with splitter plates installed.

Received May 20, 1980; revision received Sept. 29, 1980. This paper is declared a work of the U.S. Government and is therefore in the public domain.

*Aerospace Engineer. Associate Fellow AIAA.

were located on the splitter plates. The sabot was brass and had cylindrical inner and outer surfaces of radii 25.4 and 76.2 mm, respectively. The leading edge of the sabot had a 40 deg chamfer. Fifty pressure orifices were located on the chamfer, inner cylindrical surface, and side planes of the sabot component. Pressures were measured at a scani-valve transducer external to the tunnel.

Tests were conducted in the High-Speed Leg of the NASA Langley Unitary Plan Facility. The projectile was mounted on a sting extending from a window blank, while the sabot was mounted on the main traveling sting centered in the tunnel. This arrangement precluded the acquisition of schlieren or shadowgraph optics. The geometry of the 4×4 ft test section and model arrangement permitted the sabot component to move relative to the projectile over an angular range of 0-15 deg in pitch and laterally from 3.2 to 114 mm. This range is sufficient to simulate the strong aerodynamic interaction regions of interest.

Tests were conducted at a Mach number of 4.5 which is representative of actual projectile flight Mach numbers; however, flight Reynolds number was not duplicated (see Table 1). In the initial formulation of the test, this failure to duplicate free-flight Reynolds number was not considered serious, i.e., the main emphasis was on the inviscid flow structure. Unfortunately, the test results show regions of shock/boundary-layer interaction and separated flow having strong influences during the early phases of sabot discard.

A variety of combinations of components were tested. These include: sabot alone, single sabot component and projectile (with and without splitter plates), and three sabot components. Some of the data were taken to examine the effects of asymmetry in the discard pattern upon the flow properties; however, for the present discussion, only the symmetric data will be addressed.

Test Results

Sabot Alone

The instrumented sabot component was tested signly in order to obtain data on the free-flight aerodynamics of the shape. Surface pressure data along the plane of symmetry of the sabot component are given for angles of attack of 0, 8, and 16 deg in Fig. 4. As would be expected, the pressure on the front chamfer surface is high; however, it shows relatively small variation with angle of attack. The predictions of simple Newtonian theory are considerably below the measured values and show a much wider change with pitch. On the underside of the sabot, the pressures are significantly lower, reflecting the effects of expansion around the corner. The Newtonian predictions are better in this region.

Also shown on the figure is the pressure variation predicted by a semiempirical shock expansion theory suggested by Siegelman.[6] This model assumes the flow has a stagnation point at the leading edge with a sonic point at the corner followed by a Prandtl-Meyer expansion through an angle of 40 deg. The pressure distribution on the front chamfer is linearly interpolated between the stagnation pressure behind a normal shock and the associated sonic pressure. The pressure on the underside is simply assumed constant. While this model produces a good picture of the flow within the range of angle of attack, it is not sensitive to change in this angle.

Symmetry Analysis

In order to examine the effectiveness of the splitter plates in generating a flow similar to that with three sabot components, tests were conducted with the three components arranged in a fixed geometry. These results are compared with the results with splitter plates installed.

The test arrangement is shown in Fig. 3. Two additional sabot components are attached to the sting supporting the projectile. The third, instrumented sabot is supported on the main traversing sting. The sabot components are positioned at zero pitch relative to the projectile and at a lateral separation of 0.75 d. This separation was selected since preliminary analysis indicated that the area between the bodies would be sufficient to pass all of the mass flow captured by the entrance area defined by the outer edge of the sabot components. This is analogous to the starting (or normal shock swallowing problem) of a supersonic inlet. For the splitter plate tests, the positioning of the single sabot component was identical to that described above.

The pressure distributions measured on the projectile and sabot component are compared in Fig. 5. The two sets of data agree qualitatively quite well. The peak pressure on the projectile surface is due to the impingement of the shock wave off the sabot. In both cases its location is identical; however, with three sabots present, the peak is higher than that measured with the splitter plates, whereas, the level of the pressure plateau ahead of the peak is lower in the three-sabot data. These variations are due to the increased viscous effects associated with the splitter plates. The plates have boundary layers on their surfaces and develop a corner flow at intersection with the body. These types of flows have been

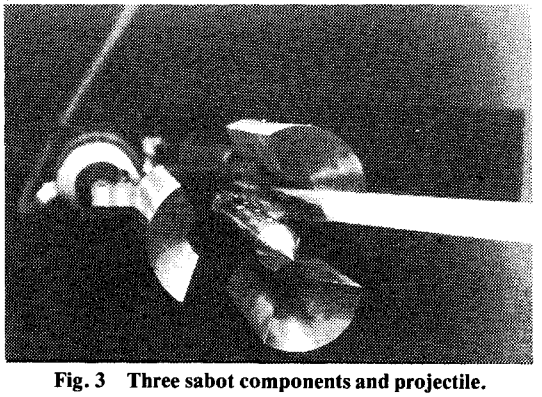

Fig. 3 Three sabot components and projectile.

Table 1 Comparison of test and flight conditions

Test	M_∞	Re/m	T_{s_∞} K,	P_{s_∞}, N/m^2
Wind tunnel	4.5	6.6×10^6	353	2.45×10^5
Free flight	4.5	8.9×10^7	1487	2.93×10^7

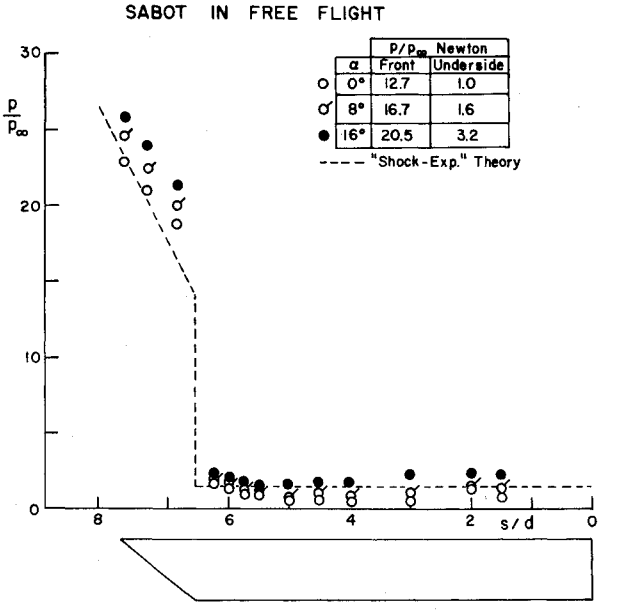

Fig. 4 Variation in presure distribution along centerline of sabot with sabot mounted independently in wind tunnel.

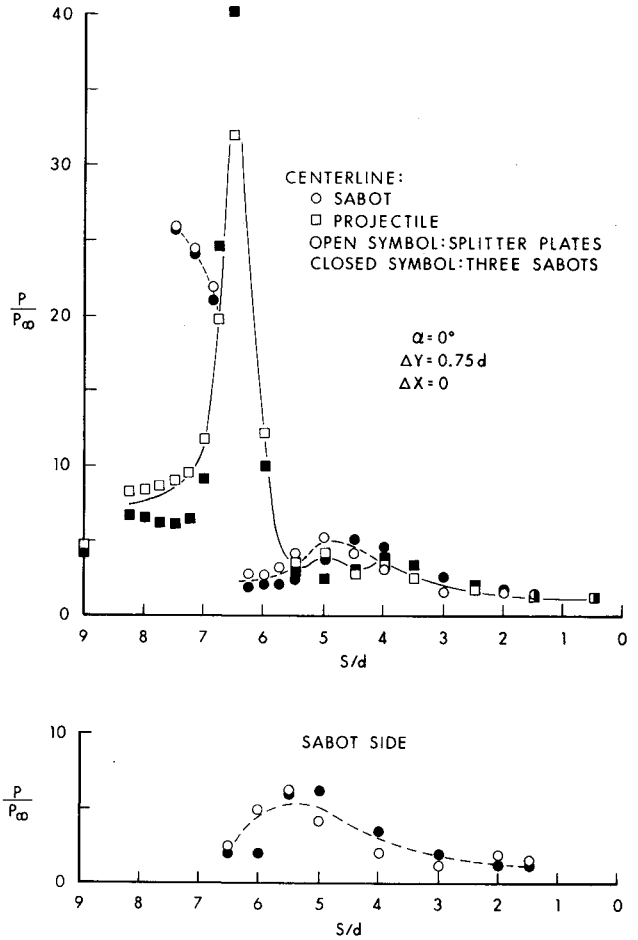

Fig. 5 Pressure distributions along centerlines of sabot and projectile for symmetry check cases.

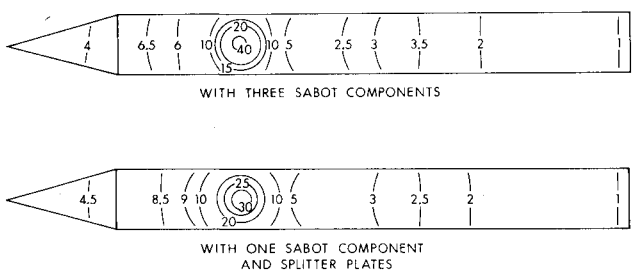

Fig. 6a Pressure contours on projectile surface for symmetry check case.

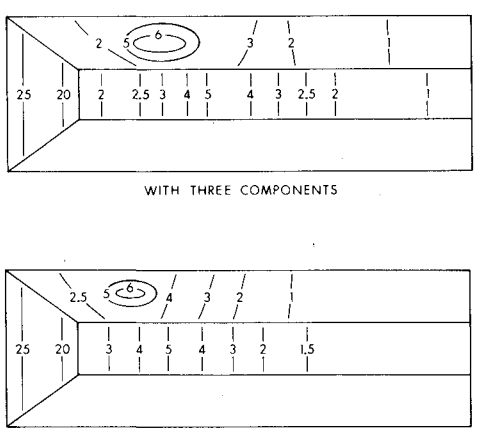

Fig. 6b Pressure contours on sabot surface for symmetry check case.

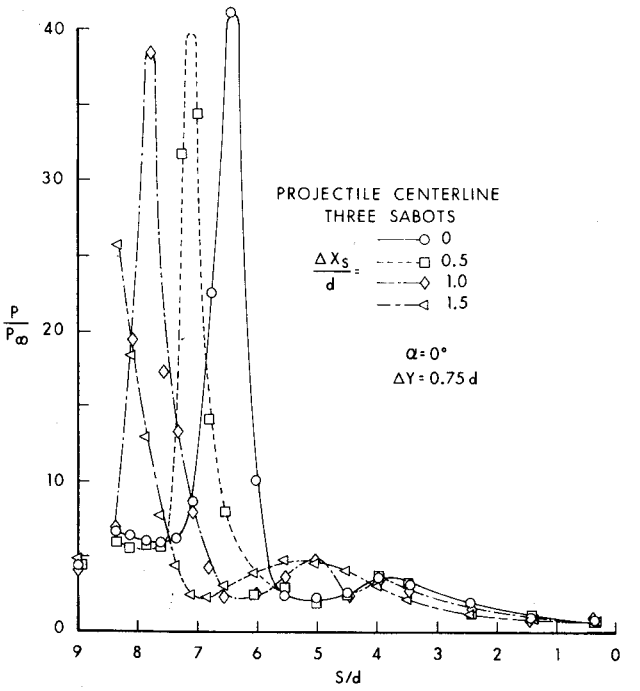

Fig. 7a Projectile centerline pressure distribution with three sabots installed (one of which is being traversed forward).

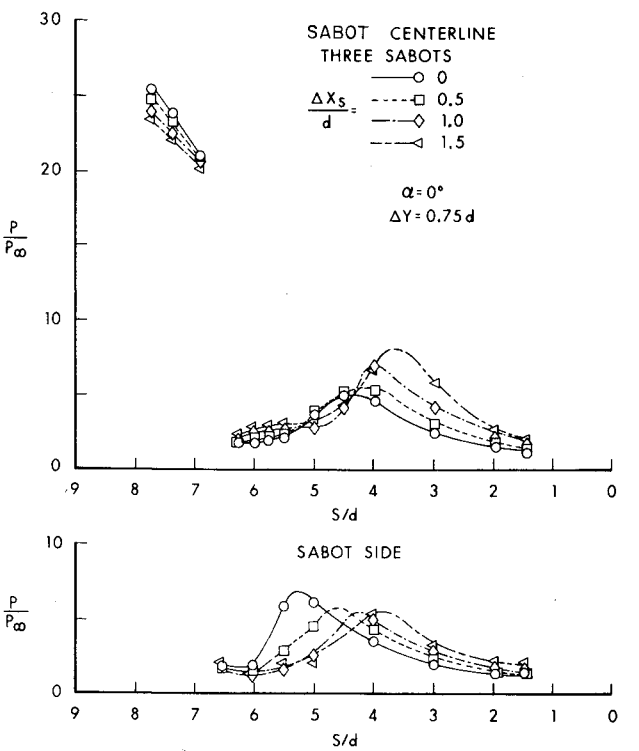

Fig. 7b Sabot pressure distribution on moving sabot with three sabots installed.

demonstrated to interact with entracne shocks on the sidewalls of two-dimensional supersonic inlets.[7] In the present case, the viscous effects associated with the splitter plates thicken the boundary layer on the body and extend the shock/boundary-layer interaction region downstream from the intersection point while reducing the height of the peak. In view of the pressure levels, it seems likely that the boundary layer has separated; however, correlated oil flow and heat-transfer data would be needed to confirm this fact.

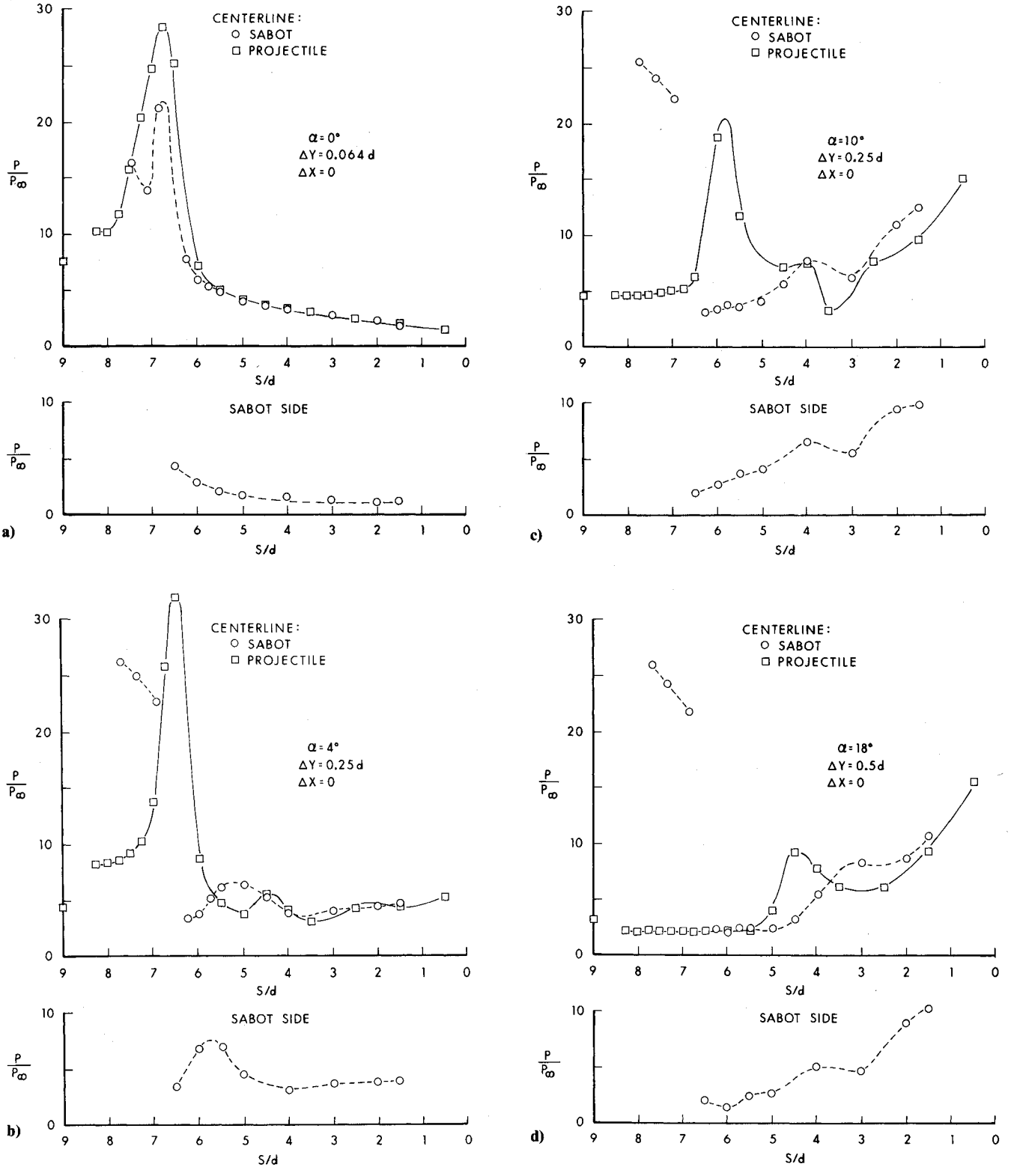

Fig. 8 Pressure distributions during simulated sabot discard.

As previously noted, the rapid rise in pressure on the projectile surface is associated with the impingement of the sabot shock wave. The equally rapid decay of this pressure peak is due to the arrival of the corner expansion from the sabot. The decay of pressure on the projectile surface is similar in both test cases.

The pressure on the front chamfer of the sabot is nearly identical in both cases. On the underside and lateral side of the sabot component, a compression occurs near $S/d=5$. The peak values are similar in both cases; however, the location is further downstream in the case of the three-sabot arrangement. Pressure contours have been constructed from the measurements in these tests and tend to emphasize the strong qualitative agreement between the two flows (Fig. 6).

Based upon a comparison between the test data in the case with three sabot components installed and that with a single sabot component and splitter plates, it is felt that while exact quantitative agreement is not achieved due to greater viscous interactions observed with the splitter plates installed, sufficiently good qualitative comparison is developed to con-

clude that the test technique is valid within the approximations and limitations of any scale-model wind-tunnel experiment.

Wave Form Analysis

The three-sabot configuration provides an opportunity to investigate the origin of some of the pressure pulses measured on the projectile and sabot surfaces. Since one of the sabot segments can be moved while the others remain fixed, it is possible to infer the shock structure from changes in the surface pressure distributions measured as the sabot segment is moved.

With the two fixed sabot segments set at zero pitch and a separation of 0.75 d, the movable component was traversed axially over a range of 1.5 d in the forward direction. The resulting surface pressure distributions on the projectile and sabot component (which is being moved) are shown in Fig. 7. As the sabot component is moved forward at 0.5 d increments, the peak pressure on the projectile surface moves forward at similar increments. This indicates that the peak is associated to the shock wave from the moving sabot component. However, examination of the pressure distribution on the moving sabot component shows that as this component moves axially forward, the peaks on the underside and lateral side move rearward a similar amount relative to the sabot. This indicates that peaks are, in part, associated with adjacent, fixed sabot components. It is interesting to note that the pressure on the underside increases as the sabot component moves forward while that on the lateral side decreases. This may be due to a tendency to develop a shock coalescence on the underside between the reflected shock from the body and the transmitted shocks from adjacent sabot components.

Sabot Discard Sequence

From the measurements taken within the text matrix, a set of data is selected which represents the range of sabot geometries in an actual discard sequence (Fig. 8).

At the closest gap distance, $\Delta Y = 0.064\ d$, and zero pitch angle, the pressure distribution shows signs of a stagnation region within the sabot front chamfer followed by a nearly one-dimensional expansion of the flow through a sonic point at the sabot corner. At the free-flight Mach number, the following flow properties may be computed:

at $M_\infty = 4.5$,

$$P_{t_2}/p_\infty = 26.5$$

$$p_2^*/p_\infty = 14.01$$

on a 15 deg half-angle cone,

$$p_c/p_\infty = 3.23$$

on a 40 deg wedge,

$$p_w/p_\infty = 19.6$$

Comparison of some of these values with the pressure levels measured on the sabot and projectile (Fig. 8a) indicates that even on the surface of the cone, $S/d = 9$, the flow is altered by the shock/boundary-layer interactions and flow separation. The excursions in pressure on the front chamfer of the sabot may be one of a variety of shock on shock interactions between the projectile and sabot shocks.[8]

As the sabot moves away from the body, the nature of the flow changes (Fig. 8b). The leading edge of the sabot is now in relatively undisturbed flow. The pressure variation across this front chamfer surface is similar to that measured with the sabot mounted independently (Fig. 4). The conical forebody of the projectile still exhibits pressure in excess of the conical flow prediction (the relaxation to this value does not occur until the furthest separation of this sequence). The cylindrical surface of the projectile shows the impingement of the sabot shock and subsequent peaks associated with successive shock reflections. The underside of the sabot is behaving in a manner similar to the flow model described by Siegelman.[6] There is apparently a sonic point at the shoulder followed by a Prandtl-Meyer expansion and arrival of the reflected and transmitted shocks from the projectile and adjacent sabots.

With increased pitch, the sabot bow shock impinges further aft on the projectile and the peak pressure decays (Figs. 8c and 8d). A strong recompression develops toward the rear of both the projectile and sabot. This may be due to the formation of a normal shock similar to the terminal shock in a supersonic inlet. Alternatively, it could represent a quasi-isentropic compression of the convergent supersonic flow channeled by the sabot components.

Experimental results show that the peak pressure on the sabot moves aft as it pitches away from the projectile. With the sabot designs typified by Fig. 1, the resulting lateral lift from these elevated pressures is not maximized because the surface area decreases along the rear ramp. In an attempt to utilize the interference loadings to assist discard, a sabot was fabricated with thin aerodynamic surfaces (wings) on the rear of the ramp. The rounds were fired in a ballistic range and discard measured using sequential x rays. The resulting angle of separation between the projectile and sabot component trajectories was increased from 2.1 to 3.8 deg. This increase in the rate of separation produces a 55% decrease in the length of the trajectory over which aerodynamic interaction can occur between the sabot components and the projectile.

Summary and Conclusions

A series of wind-tunnel tests have been conducted at NASA Langley Unitary Plan Facility to examine the aerodynamics associated with sabot discard at hypersonic Mach numbers. The data were limited to surface pressure measurements. To simulate the symmetric separation of three, nonrolling sabot components, a splitter plate technique was used which produced excellent qualitative agreement with the multiple-component baseline. Quantitatively, the effects of increased viscous interactions due to the splitter plates altered the exact pressure levels.

Tests indicated that simple Newtonian theory is not adequate, even for a single sabot component in independent free flight. The effects of shock/boundary-layer interaction are quite important. The experimental results suggested a design modification which was successfully demonstrated in hardware tests.

In order to define the flowfield better, additional testing is required with improved instrumentation. Since the projectile and sabot components form a spiked nose body when assembled, transient pressures should be measured to determine if oscillatory flow typical of such configurations occurs. Surface flow visualization would better define the nature of shock/boundary-layer interaction. Selected probing of the boundary layers and flowfield could add important definition to the flow structure. With regard to the model geometry, a variety of representative sabot shapes should be examined to determine sensitivity to the number of segments, leading-edge configuration, and lifting surface placement. Finally, the primary goal of these tests was to investigate the flow around the sabot in order to improve discard properties; thus, no attempt was made to survey the interactions with the projectile fins. Since this latter effect is a significant source of perturbation to the flight of the projectile, experimental determination of the properties of the interaction would be worthwhile.

Acknowledgment

The author wishes to thank the staff of the NASA Unitary Plan Facility for their assistance and suggestions during and

preceding the experimental program. Charlie Jackson, Odell Morris, William Corlett, and Garland Wilson all contributed their considerable expertise. Thanks also to Tom Young of the Naval Surface Weapons Center, White Oak, who designed and fabricated the models tested.

References

[1]Conn, H., "The Influence of Sabot Separation on the Yawing Motion of a Cone," Defense Research Establishment, Valcartier, Canada, TN 1849/70, June 1970.

[2]Glauz, W., "Estimation of Forces on a Flechette Resulting from a Shock Wave," Midwest Research Institute, R3450-E, May 1971.

[3]Schmidt, E. and Shear, D., "Aerodynamic Interference During Sabot Discard," *Journal of Spacecraft and Rockets,* Vol. 15, May-June 1978, pp. 162-167.

[4]Orlik-Ruckemann, K., "Half and Full-Model Experiments on Slender Cones at Angle of Attack," *Journal of Spacecraft and Rockets,* Vol. 11, Sept. 1973, pp. 575-580.

[5]Orlik-Ruckemann, K., "Supersonic Dynamic Stability Experiments on the Space Shuttle," *Journal of Spacecraft and Rockets,* Vol. 9, Sept. 1972, pp. 655-660.

[6]Siegelman, D. and Crimi, P., "Projectile/Sabot Discard Aerodynamics," Paper 80-1588 presented at AIAA Atmospheric Flight Mechanics Conference, Danvers, Mass., Aug. 12-14, 1980.

[7]Paynter, G., "Analysis of Weak Glancing Shock/Boundary Layer Interactions," Paper 79-0144 presented at AIAA 17th Aerospace Sciences Meeting, New Orleans, La., Jan. 15-17, 1979.

[8]Edney, B., "Effects of Shock Impingement on the Heat Transfer Around Blunt Bodies," *AIAA Journal,* Vol. 6, Jan. 1968, pp. 15-21.